APPLICATION OF OPEN BOUNDARIES WITHIN A TWO-WAY COUPLED SPH MODEL TO SIMULATE NON-LINEAR WAVE-STRUCTURE INTERACTIONS

Verbrugghe, T.[1], Domìnguez, J. M.[2], Altomare, C.[3], Tafuni, A.[4], Troch, P.[1], Kortenhaus, A.[1]

A two-way coupling between the fully non-linear potential flow (FNPF) solver OceanWave3D and the Smoothed Particle Hydrodynamics (SPH) solver DualSPHysics is presented. At the coupling interfaces within the SPH domain, an open boundary formulation is applied. An inlet and outlet zone are filled with buffer particles. At the inlet, horizontal orbital velocities and surface elevations calculated with OceanWave3D are imposed on the buffer particles. At the outlet, horizontal orbital velocities are imposed, but the surface elevation is extrapolated from the fluid domain. Velocity corrections are applied to avoid unwanted reflections in the fluid domain. The SPH surface elevation can be coupled back to OceanWave3D, where the original solution is overwritten. The coupling methodology is validated using a 2-D test case of a floating box. Additionally, a 3-D proof of concept is shown where overtopping waves are acting on a heaving cylinder. The 2-way coupled model proofs to be capable of simulating wave propagation and wave-structure interaction problems with an acceptable accuracy with RMSE values remaining below the smoothing length h.

Keywords: Smoothed Particle Hydrodynamics; Open Boundaries; Coupling

INTRODUCTION

Smoothed Particle Hydrodyanmics (SPH) methods typically are computationally very intensive. However, recent advances using HPC and GPU have strongly contributed to significant gains in computational effort (Gotoh and Khayyer, 2018). Despite the use of HPC and GPUs, it is still challenging to model real engineering problems, which are usually multi-scale problems. An alternative to optimizing SPH for powerful computing hardware, is to study possible reduction of the computational domain. This can be done by coupling SPH to a faster external numerical model. This requires accurate and stable boundary conditions. Both the development of accurate boundary conditions and the coupling of SPH to external models are part of the SPHERIC Grand Challenges `http://spheric-sph.org/grand-challenges`. In literature, there are several research examples where coupling was applied within SPH. A general algorithm for one-way coupling of SPH with an external solution has been proposed in Bouscasse et al. (2013). The interaction between the SPH solver and the external solution is achieved through an interface region containing a ghost fluid, used to impose any external boundary condition. In Fourtakas et al. (2018), A hybrid Eulerian-Lagrangian incompressible SPH formulation is introduced, where two different SPH formulations are coupled rather than two completely different solvers. The SPH solver DualSPHyics has been coupled in Altomare et al. (2016) and (2018), where a one-way coupling was realized with the wave propagation model SWASH. A numerical wave flume has been created to simulate wave impact and run-up on a breakwater. The first part of the numerical flume is simulated using the faster SWASH model, while the wave impact and run-up are calculated using DualSPHysics. Here, a one-way coupling is sufficient, since there is only interest in the impact of waves on the breakwater. In Kassiotis et al. (2011), a similar approach has been adopted, where a 1-D Boussinesq-type wave model is applied for wave propagation in most of the spatial domain, and SPH computations focus on the shoreline or close to off-shore structures, where a complex description of the free-surface is required. In Narayanaswamy et al. (2010), the Boussinesq model FUNWAVE was coupled to DualSPHysics, where the key development was the definition of boundary conditions for both models in the overlap zone. A wave generator in SPH moved according to the velocities from the adjacent Boussinesq nodes. Similarly, an incompressible SPH solver has been coupled to a non-linear potential flow solver QALE-FEM in Fourtakas et al. (2017). In Chicheportiche et al. (2016), a one-way coupling between an potential Eulerian model and an SPH solver is realised, applying a non-overlapping method using the unsteady Bernoulli equation at the interface. These studies applied coupling to speed up the simulation time by minimizing the computationally intensive SPH domain. Other studies apply coupling to combine both the benefits of mesh-based and mesh-free CFD methods. In Didier et al. (2013), the wave propagation model FLUINCO is coupled to an SPH code, and validated with experimental data of wave impact on a porous breakwater. A hybrid multiphase OpenFOAM-SPH model is presented

---

[1]Department of Civil Engineering, Ghent University, Belgium
[2]EPHYSLAB Environmental Physics Laboratory, Universidade de Vigo, Spain
[3]Flanders Hydraulics Research, Belgium
[4]School of Applied Engineering and Technology, New Jersey Institute of Technology, USA

in Kumar et al. (2015), where the SPH method is used on free surfaces or near deformable boundaries whereas OpenFOAM is used for the larger fluid domain. A similar coupling is used, where breaking waves are modelled with SPH and the deeper wave kinematics are modelled with a FV method. This has been demonstrated in Marrone et al. (2016) for a weakly-compressible SPH (WCSPH) solver and in Napoli et al. (2016) for an incompressible SPH (ISPH) solver. This research focuses on applying open boundaries in a 2-way coupling methodology between the fully non-linear potential flow (FNPF) solver OceanWave3D and the SPH solver DualSPHysics.

Typically, SPH domains for wave propagation modelling are at least 3-4 wavelengths long (Altomare et al., 2016). Combined with a required small particle size to accurately reproduce the surface elevation, this leads to computationally intensive simulations. This research is aimed at reducing the necessary fluid domain, and provide accurate boundary conditions capable of active wave generation and absorption by applying a coupling with the wave propagation model OceanWave3D. In this manner, real open sea conditions can be simulated where waves enter at the left-hand-side of the fluid domain and exit freely at the right-hand-side. The WCSPH model DualSPHysics will be used to demonstrate the coupling methodology, using the recently developed open boundaries (Tafuni et al., 2016, 2017, 2018). The applied open boundary formulation is based on the use of buffer layers adjacent to the fluid domain. Buffer particles are used to enforce certain conditions in presence of fluid inlets and outlets. Particularly, the physical information of buffer particles is either assigned a priori or extrapolated from the fluid domain using a first order consistent procedure. The major benefits of this method are:

- Using open boundaries for wave generation and absorption is meant to cover those cases where classical wave generation techniques can fail or are very computationally expensive, e.g. open sea states, simulating floating devices, wave breaking conditions, ...

- The buffer zones in the open boundaries accept physical information from any source: e.g. linear wave theory, non-linear wave theories, external numerical models such as CFD models, or even measurement data.

OPEN BOUNDARIES WITHIN DUALSPHYSICS

Within this research, open boundaries are applied to generate and absorb waves. The implementation of open boundaries in DualSPHysics is discussed in detail in Tafuni et al. (2018). Inflow and outflow buffers can be defined near the inlets and outlets of the computational domain. Flow conditions can be either imposed or extrapolated from the domain interior using ghost nodes. In the latter case, variables at the ghost nodes are first calculated via a standard particle interpolation and then corrected to retrieve first order consistency. Finally, they are mirrored back to the boundary particles using Taylor series approximations.
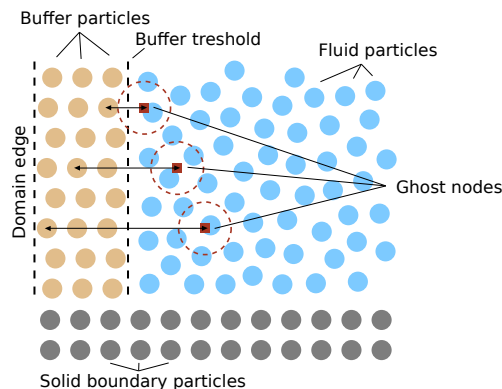
Figure 1: Sketch of the implemented open boundary model, adapted from Tafuni et al. (2018).

A sketch of the implemented boundary condition model is shown in Figure 1 in the generic case of a fluid flowing near a buffer area identifying an open boundary. The buffer zone is situated in between the domain edge and the buffer threshold boundary, i.e. the fluid-buffer interface. The zone is filled with layers of SPH buffer particles used to enforce certain boundary conditions. The buffer size should be at least equal

to or exceed the kernel radius. This is necessary to have full kernel support for the fluid particles near an inlet or outlet. In the present research, the buffer width is chosen as $8 \cdot d_p$ in the direction normal to the open boundary, where d_p is the particle size adopted in DualSPHysics. Providing the information to an open boundary is possible using two methods: physical quantities are either assigned a priori or extrapolated from the fluid domain to the buffer zones using ghost nodes. As illustrated in Figure 1, the positions of the ghost nodes are calculated by mirroring the buffer particles into the fluid along a direction normal to the open boundary.

The open boundary algorithm introduces several new features that make SPH more applicable to real engineering problems. The first one is the possibility of using buffer areas to impose unsteady velocity and pressure profiles, as well as pressure and velocity gradients along a chosen direction. Next, a variable free-surface elevation can be imposed, which is an essential prerequisite in free-surface flow problems where waves can enter and exit the computational domain. Finally, the buffer areas are characterised by a dual behaviour, allowing both inward and outward flows, making flow reversion possible. Consequently, when flow velocities are extrapolated from the fluid domain, mixed velocity fields are possible where part of the buffer area contains fluid particles entering the domain, and another part contains fluid particles leaving the domain. This can be specifically important when flow problems with strong rotations or oscillations need to be modeled. This flexibility is an important distinctive feature. Since the open boundary algorithm is available on both the parallel CPU and GPU versions of DualSPHysics, considerable speed-ups can be achieved when running the code on high-end GPUs or large CPU clusters. This is particularly necessary when simulating real engineering problems where a large number of particles is necessary to study high-resolution flow problems with complicated geometries, while maintaining a reasonable computation time.

COUPLING METHODOLOGY

As mentioned before, SPH simulations are very computationally intensive. The data output required from a WEC SPH model is often limited to a zone closely spaced around the floating WEC. However, there is a spatial need for wave generation and wave absorption, around $3 - 4$ wavelengths long. This leads to a significant increase in water particles, and thus higher computation times. Moreover, wave generation techniques available in DualSPHysics are limited to first and second order wave generation by using piston-type or flap-type wave paddles. This generation type requires a certain propagation length before the full kinematics and surface elevation are developed. Within this research, the objective is to simulate higher-order (up to 5th) irregular short-crested waves in a domain which is as small as possible. In an attempt to answer both the problem of computational performance and the problem of wave generation, a coupling methodology as illustrated in Fig. 2 is developed.

Table 1: **Imposed and extrapolated quantities for inlet and outlet buffer particles (Imp=imposed, Ext=extrapolated, Hyd=hydrostatic).**

Quantity	u	w	η	p
inlet	Imp	0	Imp	Hyd
outlet	Imp	0	Ext	Ext

Here, a fluid domain with a length of 1 wave length is chosen, with an inlet at the left-hand-side of the domain and an outlet at the right-hand-side of the domain (see Figure 2). Each buffer zone consists of 8 layers of buffer particles. A sensitivity analysis has shown that wave propagation results are accurate for buffer zones with at least 8 layers. The imposed physical quantities originate from non-linear wave theory. At the inlet, theoretical horizontal orbital velocities and surface elevation are imposed on the buffer particles, while the pressure is set to be hydrostatic. At the outlet, only the horizontal orbital velocities are imposed, the surface elevation and pressure are extrapolated from the fluid domain (see Table 1). No vertical orbital velocities are applied, analysis has proven that there is no accuracy benefit by imposing vertical velocities, but there is a negative impact on particle spacing.

By imposing horizontal velocities on both the inlet and outlet, the hydrodynamic problem becomes over-constrained, which can result in unwanted reflections in the fluid domain. Additionally, when a floating or fixed structure is positioned in the fluid domain, waves will reflect on the structure and transform around
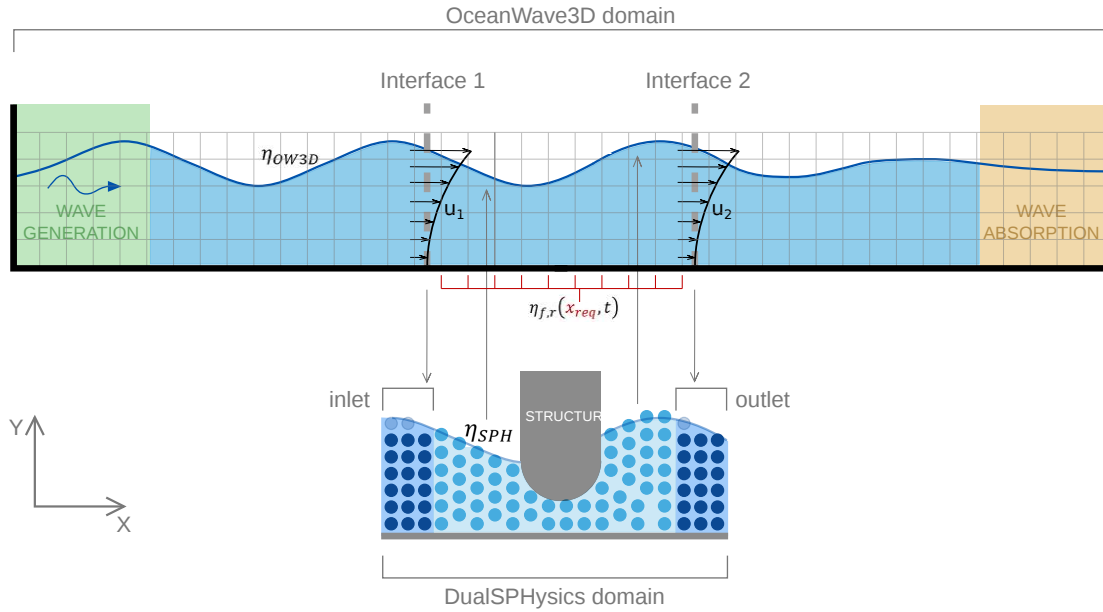
Figure 2: General sketch of coupling methodology between OceanWave3D and DualSPHysics.

it. The open boundaries should be able to compensate for the reflected waves and the outlet needs to absorb the transformed wave effectively. In this research, this is done by applying velocity corrections at the inlet and the outlet, based on the measured free surface close the buffer interface, specifically at a distance of $8 \cdot d_p$. This distance has been selected based on a sensitivity analysis. At a distance of $8 \cdot d_p$, the wave measurement location is close enough to the buffer zone to have a minimal phase difference, but far enough to avoid inaccuracies due to transitional effects between the buffer zone and the fluid domain. In Figure 2, these measuring locations are denoted as WG_{in} (Wave Gauge) and WG_{out}. The applied velocity correction is a shallow water wave correction based on the measured reflection (Dean and Dalrymple, 1991), but is implemented differently depending on the inlet or the outlet.

Inlet Velocity Correction

At the inlet, the objective is to always generate the required incident wave. The surface elevation is measured directly outside of the inlet, and the velocity is corrected to ensure that the generated surface elevation matches the theoretical one. In case a higher surface elevation is measured than what was imposed, the corrected velocity should be lower than the originally imposed profile, in order to compensate the excess of velocity, since that profile leads to reflections in the fluid domain. Within the code, this correction is implemented as follows:

$$u_{in}(z,t) = u_{theory}(z,t) - \left[\eta_{WG,in} - \eta_{theory} \right] \cdot \sqrt{\frac{g}{d}} \tag{1}$$

Here, u_{in} is the horizontal velocity at the inlet, u_{theory} is the imposed horizontal velocity, $\eta_{WG,in}$ is the measured free surface elevation near the inlet, η_{theory} is the imposed free surface, g is the earth's acceleration and d is the water depth. This correction is similar to the active wave absorption applied in Altomare et al. (2017), although there it was used to correct the displacement of a piston-type wavemaker formed by moving boundary particles.

Outlet Velocity Correction

At the outlet, the objective is to absorb any wave propagating towards the outlet. Technically, the applied open boundaries do not absorb the wave, but rather try to match the velocity field present in the fluid domain as close as possible, creating an 'open door' for the propagating wave. The surface elevation is measured directly outside of the outlet, and the velocity is corrected to ensure that the imposed velocities match the measured ones. In case a higher surface elevation is measured than what was imposed, the corrected velocity should be higher than the originally imposed profile, in order to prevent discontinuities

in the velocity field, which would induce unwanted reflected waves into the domain:

$$u_{out}(z,t) = u_{theory}(z,t) - \left[\eta_{theory} - \eta_{WG,out}\right] \cdot \sqrt{\frac{g}{d}} \tag{2}$$

Coupling Algorithm

The coupling algorithm is illustrated in Figure 3, where a schematic representation of the algorithm during one coupling time step is given. The coupling communication occurs at the beginning and at the end of an OceanWave3D timestep, which we will call the communication time step. At the beginning of a time step, the horizontal orbital velocities at the inlet and outlet locations, $u_{in/out}$, are calculated in OceanWave3D, as well as the surface elevation of the complete OceanWave3D domain η_{OW3D}, and sent to a Python program using the MPI protocol. Simultaneously, Python receives the measured surface elevation from DualSPHysics near the inlet and outlet $\eta_{WG,in/out}$. The velocity correction is calculated and the corrected orbital velocities $u_{in/out,C}$ are sent back to DualSPHysics, together with the surface elevation at the inlet η_{in}. The quantities are imposed within the inlet and outlet and the DualSPHysics simulation continues until the communication time step is finished. The surface elevation from DualSPHysics is sent to Python, where the signal is filtered and sent back to OceanWave3D as η_{new} to overwrite the original result.
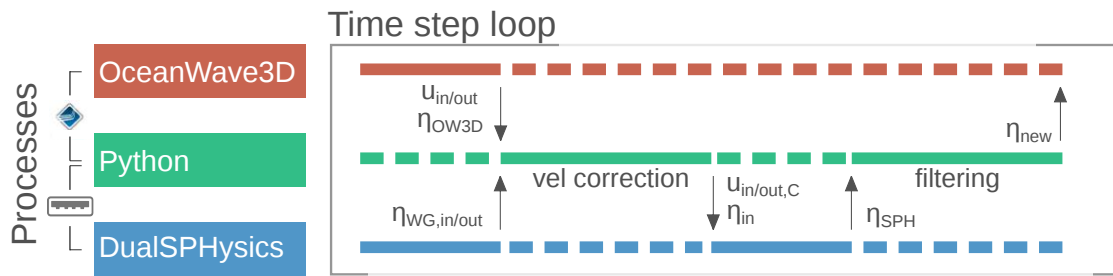

Figure 3: Redesigned coupling algorithm

2D VALIDATION

First, the 2-way coupling with OceanWave3D is validated in 2-D. The coupled model is applied to compare the response of a floating box to experimental data, as described in Ren et al. (2015). The experimental and numerical test set-up is illustrated in Figure 4. The full wave propagation domain has a length of 20.0 m. The floating box is positioned at $x = 5.5\ m$ and has the dimensions 0.3 m x 0.2 m (LxH) with a draft of 0.1 m. The water depth is 0.4 m, while the DualSPHysics domain is 6.12 m wide (3 wave lengths) and starts at $x = 4.0\ m$. A regular wave with wave height $H = 0.1\ m$ and wave period $T = 1.2\ s$ is generated, characterised as a Stokes third-order wave. A particle size of $d_p = 0.01\ m$ is used. The SPH domain is chosen to be larger than one wavelength, since the box is freely floating and will drift in the x-direction over time.
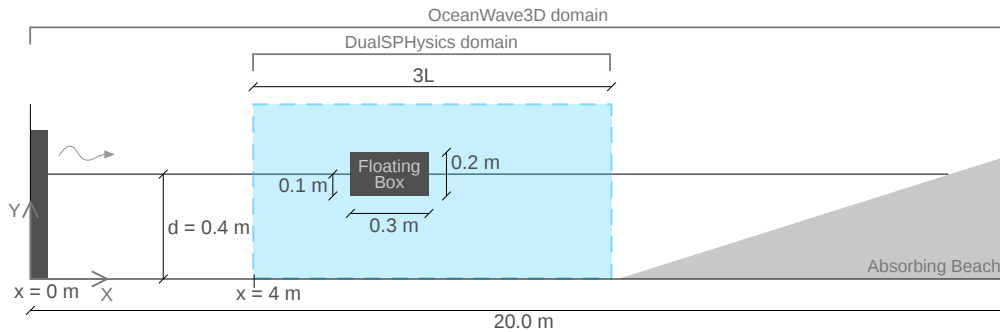
Figure 4: Experimental and numerical test set-up for simulation of the response of a floating box to a custom wave signal. The DualSPHysics domain and OceanWave3D domain are indicated.
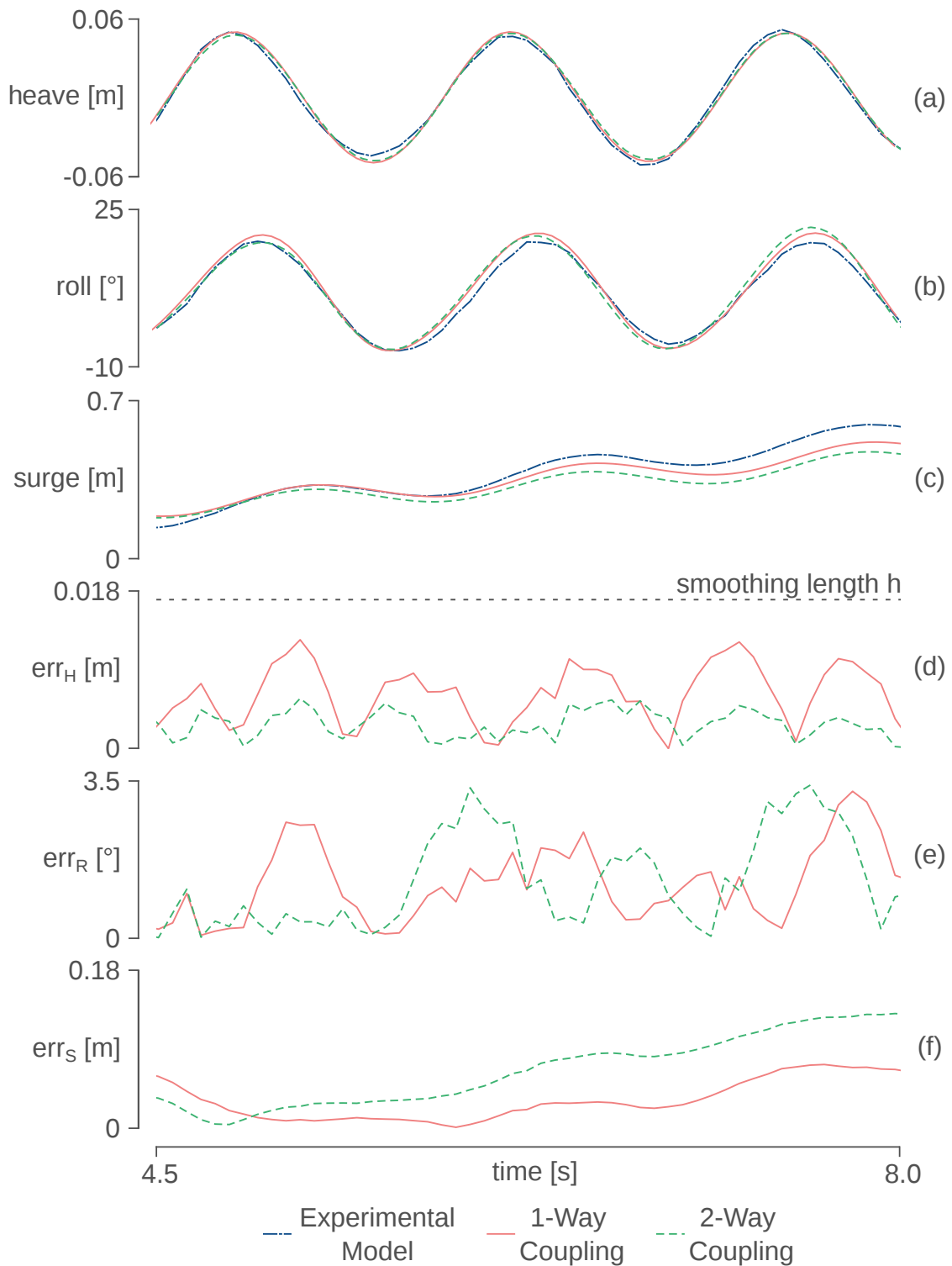
Figure 5: Comparison of time series and error between numerical and experimental results of the 3 degrees of freedom of the box with heave, roll and surge motions.

Results and discussion

Both a one way coupling and two-way coupling are compared to the experimental data, and the corresponding errors are illustrated in Figure 5. In the one-way coupling, OceanWave3D only provides the horizontal orbital velocities to the inlet and outlet zone, and the surface elevations for the inlet and the calculation of the velocity corrections. For the two-way coupling, the surface elevations from the DualSPHysics domain are transferred back to the OceanWave3D domain, where the original solution is overwritten. The zone close around the floating box is not coupled back, since the 'measured' SPH free surface elevations are not physical there. A good correspondence between the numerical and experimental results is shown. Specifically the heave and roll motions are accurately reproduced. The error on the heave motions remains well below the smoothing length $h = 0.017\ m$ while the roll error stays below 3.5 degrees. Although the cyclic surge path is also visible in the numerical results, the net drift in the x-direction is less accurately modelled. Logically, the error on the surge motion becomes larger in time.

Additionally, the surface elevation profile at $t = 15\ s$ of DualSPHysics and OceanWave3D is compared in Figure 6. Three wave profiles are plotted. For the two-way coupling methodology, both the OceanWave3D and DualSPHysics profile are plotted. Normally, these lines are expected to be exactly the same, since the original OceanWave3D surface elevation is overwritten. However, as described before, relaxation functions are applied to ensure a smooth transition between the OceanWave3D solution and the DualSPHysics solution. In Figure 6, this is visible where only close to the masked out zone both solutions match perfectly. Behind the masked out zone, both solutions remain the same until they slightly differ again at the boundary of the SPH zone. As a reference, the OceanWave3D solution for a one-way coupling is shown as well. Here, there is no influence from the DualSPHysics solution, and OceanWave3D propagates waves as if there is no floating box present. Nevertheless, this does not impact the accuracy of the results significantly, as proven in Figure 5. Again, it can be concluded that the 2-way coupling methodology should only be applied when there is a significant wave transformation effect around the structure, present in the SPH domain.
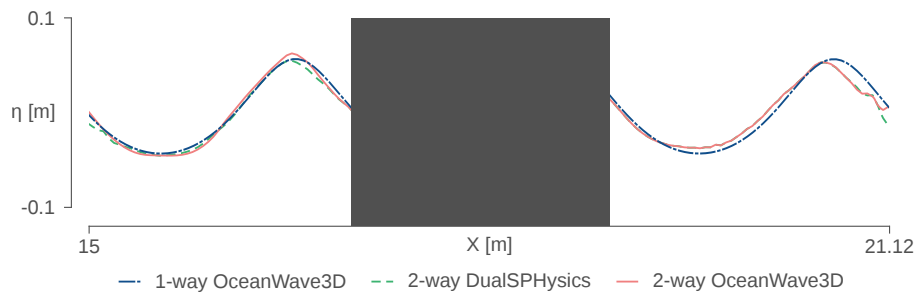
Figure 6: Comparison of wave profile between one-way and two-way coupling results of OceanWave3D and DualSPHysics. The gray masked out zone is the region around the floating box, omitted from the coupling.

3D PROOF-OF-CONCEPT

In this Section, the introduced coupling methodology is extended to a 3-D domain. A one-way coupling with a fifth-order Stokes wave theory is applied. The buffer zones are stretched in the y-direction and the imposed quantities are constant in that direction. This means 3-D simulations are restricted to long-crested waves. This means the coupling methodology can be used to model wave flume type experiments where significant 3-D effects are present. To demonstrate this, a heaving disk is simulated, impacted by steep non-linear waves. This results in non-linear wave surge forces and overtopping.

Experimental set-up

Experimental tests have been performed in the large wave flume of Ghent University (see Figure 7). The flume is 30 m long and 1 m wide. A cylindrical WEC with a diameter of 0.5 m is positioned at 10.6 m from the wave paddle. It's motion is restricted to heave by a vertical rod over which it is sliding. Friction losses are minimized by using two sets of PTFE bearings: one on the top and one on the bottom of the cylinder. The WEC consists of 10 glued plastic disks and is waterproofed with a black, MS polymer coating. Absorption material is installed at the end of the flume to ensure minimal reflections. Active wave absorption is applied using two wave gauges about 3 m away from the paddle. 7 wave gauges are installed

to measure the free surface elevation. The WEC has a diameter of $D = 0.5\ m$ and a draft of $T_{WEC} = 0.113\ m$. The motion of the WEC is captured by video tracking using a GoPro Hero 5, filming in Full HD at 120 fps. The typical fisheye distortion is corrected using video processing software. The horizontal surge force is measured by 2 force transducers, installed in a rigid rod behind the WEC to which it is connected. The incident wave has a wave height of $H = 0.12\ m$, a wave period of $T = 1.2\ s$ in a water depth of $d = 0.7\ m$. This results in a Stokes third-order wave with a wave length of $L_{wav} = 2.17\ m$.
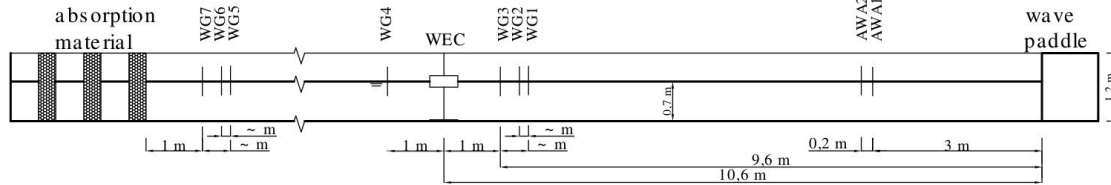
Figure 7: Experimental test set-up for modelling a heaving disk type WEC in the large wave flume of Ghent University.

Numerical set-up

The numerical set-up is illustrated in Figure 8 and summarized in Table 2. It is chosen to keep set the length of the fluid domain to twice the wave length $2 \cdot L_{wav} = 4.34\ m$. This is around 1/7 of the total flume length. The particle size is chosen to be $d_p = 0.01\ m$, which is smaller than $H/10$. The Stokes fifth-order wave theory is applied. No shifting algorithm is used since this interferes with the floating body physics. Since there is always a gap of 1.5 times the smoothing length h between fluid particles and boundary particles, the top of the floating disk is lowered with a value of $1.5 \cdot h = 1.5 \cdot 1.2 \cdot \sqrt{3 \cdot d_p^2}$, in order to get the correct overtopping height. A 3-D inlet zone and outlet zone are configured, with each 8 planes of buffer particles. All other boundaries are wall conditions with an option to extrapolate the pressure from the fluid domain, in order to avoid local pressure peaks. The WEC is positioned in the center of the domain and is restricted to allow only the heave motion.
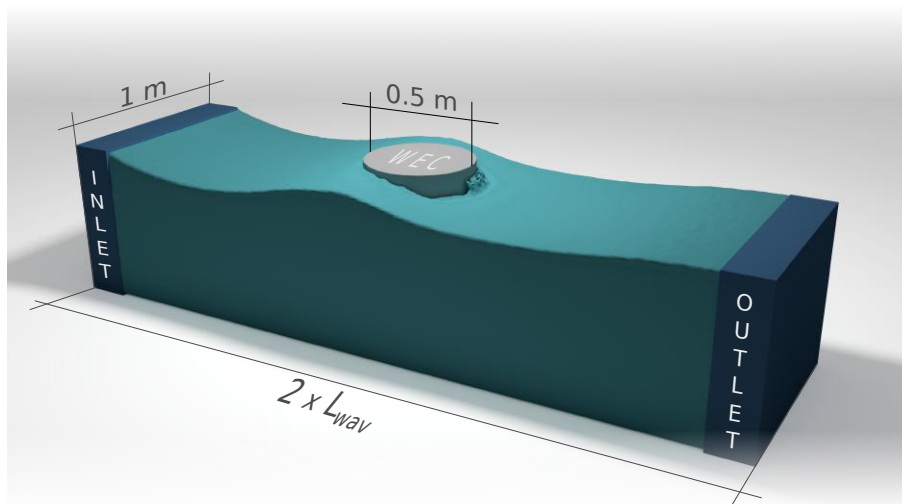
Figure 8: Numerical test set-up for 3-D modelling of a heaving cylindrical WEC in a numerical wave flume.

Results and discussion

First, the model surface elevations are compared with the experimental results. The signals from WG3 and WG4 (see Figure 7) are compared to the numerical result. WG3 is positioned 1 m in front of the WEC, WG4 1 m behind the WEC. The comparison with the data from WG3 is shown in plot (a) of Figure 2, while plot (b) shows the WG4 data. The surface elevation in front of the WEC is accurately reproduced.

Table 2: Simulation parameters for 3-D modelling of a heaving cylindrical WEC

|	
Wave Height H [m]	0.12
Wave Period T [s]	1.2
Water Depth d [m]	0.7
Wave Length L_{wav} [m]	2.17
Particle Size d_p [m]	0.01
Domain Length L [m]	4.34
Domain Width W [m]	1.0
WEC Diameter D [m]	0.5
WEC Draft T_{WEC} [m]	0.113
Wave Theory	Stokes 5th
Time Step Algorithm	Verlet
Artificial Viscosity	0.01
δ - SPH	0.1

There is some initialisation time, but after a while the wave signal is steady and matches the experimental data very well. The error remains well below the smoothing length $h = 0.017$ m. Behind the WEC the numerical results are less accurate. The coupled 3-D model predict lower wave heights behind the WEC than what was registered in real life. The measured free surface also has a steeper non-linear profile than what was calculated numerically. This could be due to the shortened SPH domain with respect to the full experimental flume length. However, the error is still acceptable since the maximum error lies around the smoothing length h.

Second, the horizontal surge force is calculated and compared to the experimental data in plot (c) of Figure 2. Here, it is clear that there is a very good match between the numerical and experimental results. Although both signals have some noise, the overall trend of the data matches very well.

Third, the comparison of the heave motion of the WEC to the experimental data is shown in plot (d) of Figure 2. Again, after initialisation of the surface elevation in the flume, a steady regime is obtained in which the calculated WEC motion and measured motion show an excellent agreement, with a maximum error of $0.4h$.

Computational Speed-up

The coupling methodology with open boundaries leads to significant performance gains with respect to typical SPH simulations. In this section, an estimation of the computational speed-up is made, comparing the presented model with a numerical model, describing the complete experimental set-up. The latter is thus an SPH simulation where the full wave flume is modelled, including the wave paddle motion and the floating disk, installed at $x = 10.6$ m. The comparison is summarized in Table 3. In the coupled model, the domain length was set at twice the wave length, resulting in a total length of 4.34 m. This is about 1/7 of the wave flume length, which explains the number of fluid particles in the full model, which is about 718 % more than in the coupled model. The difference in total number of particles is lower, at only 508 %. This is due to the thickness of the bottom boundary in the coupled model, which is thicker to allow for accurate pressure extrapolation. The difference in GPU memory is similar at 505 %, with an absolute value of 3941 MB for the full model. Although our GPU card has 8106 MB of memory available, this simulation is incredibly demanding. Computational performance is not only dependent on GPU memory, since the number of CUDA cores and their clock rate are much more indicative of simulation time. The estimated runtime, which is calculated at the start of the simulation, is significantly longer for the full model than for the coupled model. However, the difference of 411 % is slightly lower than the difference in particles. The real runtime of the coupled model was 91 hours. This remarkable difference in estimated runtime and real runtime can be explained by inaccurate estimations at the beginning of the simulation, in combination with performing other tasks on the computer, slowing down the simulation. It is chosen to not run the full model
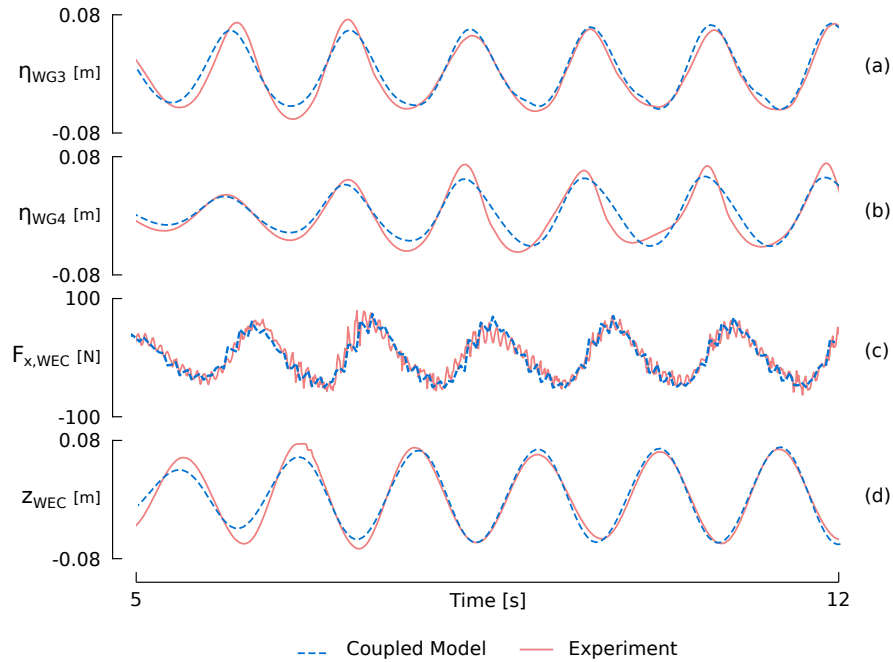
Figure 9: Comparison of 3-D proof-of-concept with experimental data of a heaving cylinder in overtopping non-linear waves. Plot (a) shows the surface elevation 1 m in front of the WEC, (b) the surface elevation 1 m behind the WEC, (c) the horizontal surge force acting on the WEC and (d) the heave motion of the WEC

Table 3: Computational speed-up for 3-D proof-of-concept

	Coupled Model	Full Model	Difference
# Particles	5 010 954	25 473 152	508 %
# Fluid Particles	2 949 433	21 165 100	718 %
GPU Memory [MB]	780	3941	505 %
Estimated Runtime [hr]	35	144	411 %
Real Runtime [hr]	91	375	411 %

completely, since the computer becomes unusable during the simulation and it could take up to 375 hours or almost 16 days to finish if the same performance as the coupled model is assumed. It is safe to assume that a speed-up of around 400 % can be achieved, by applying the coupling methodology.

Visual Comparison of overtopping

During the experiments, the steep non-linear waves are overtopping the cylindrical WEC. However, no overtopping rates or thickness of the overtopping layer were measured, so a real validation is impossible. For this reason, only a visual comparison of an overtopping event between the experiment and the numerical model is performed. In Figure 10, a time progression of an overtopping wave is shown. Here, the wave height was set at $H = 0.15\ m$ and the wave period was $T = 1.0\ s$. This resulted in steep, highly non-linear waves with significant overtopping. Also, for this test case, video images were available to perform a visual comparison. In the left plot, the wave is just about to hit the cylindrical WEC. In the middle plot, 0.4 seconds later, the overtopping wave is on top of the WEC, and in the final plot, the overtopped volume is flowing from the top back into the flume. Visually, the correspondence between the numerical model and the experimental images is very good, apart from the splash of the water against the rod, since it is not present in the numerical model.
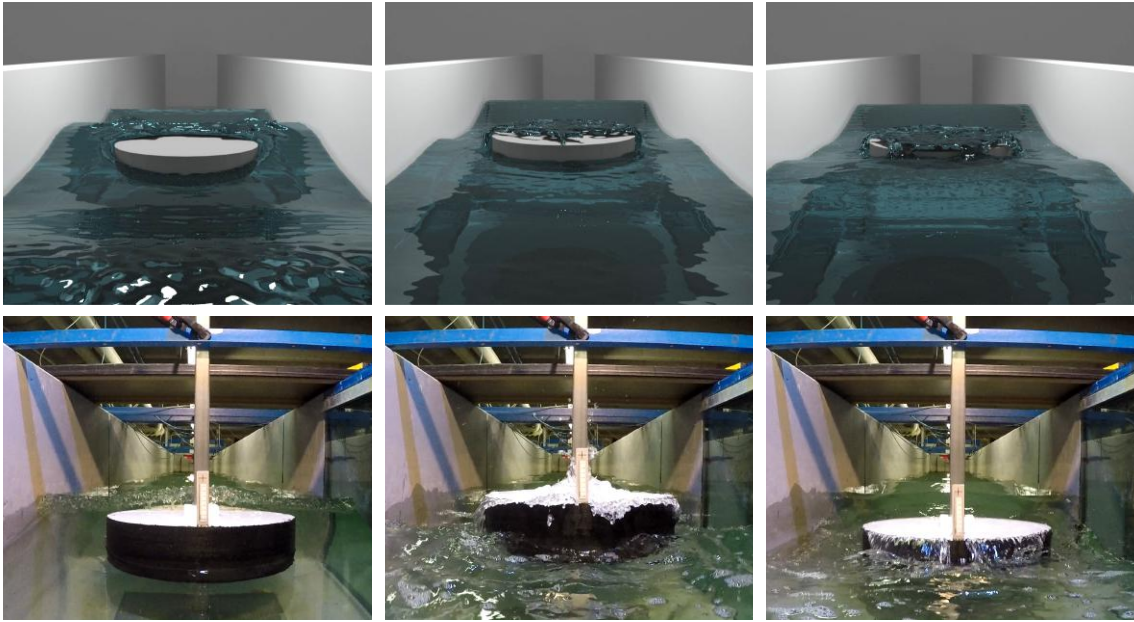
Figure 10: Visual comparison of overtopping waves between the 3-D proof-of-concept with experimental data of a heaving cylinder in overtopping non-linear waves. The plot shows a time progression of the wave, from left to right with a time difference of 0.4 s between each frame

CONCLUSIONS

A two-way coupling methodology was introduced, applying the open boundary formulation to accurately generate, propagate and absorb waves within DualSPHysics. A 2-way coupling between Python and DualSPHysics was realised to apply velocity corrections to the inlet and outlet buffer zones, to avoid reflections inside the fluid domain. The 2-way coupling methodology with OceanWave3D was validated in 2-D by comparing the motions of a floating box to experimental data. Finally, a 3-D proof-of-concept was introduced where steep non-linear waves interact with and overtop a heaving cylindrical WEC. The results all show a good agreement with the experimental data. The coupling methodology has the following benefits:

- The computation time can be significantly smaller since only a part of the full wave propagation domain is simulated in DualSPHysics. In the performed tests, the coupled model has at least 2 to 4 times less particles to simulate, which directly results into faster computation times;

- Alternatively, for the same computation time as a stand-alone SPH simulation, there is the possibility of simulating more particles for a higher accuracy.

- Due to the application of open boundaries, there are no issues with Stokes drift, and the velocity and pressure field are significantly smoother than those calculated with the coupling methodology applying moving boundaries.

However, there are still a number of limitations to this revised coupling methodology. Firstly, only quasi-3D simulations are possible. The buffer zones do not allow non-uniform velocities or surface elevations along the y-directions. This means the 3-D simulations are limited to long-crested waves. However, this can already be very meaningful to simulate typical wave flume experiments, or real engineering problems where there is not much variability in the y-direction. The numerical stability in 3-D simulations needs to improve. The open boundaries still have some compatibility issues with the periodic boundary conditions within DualSPHysics and with the boundary pressure extrapolation algorithm. Although good results are obtained, there is a certain loss of particles during the simulations. This will however be solved within future releases of the source code.

References

C. Altomare, J. M. Domínguez, A. J. C. Crespo, T. Suzuki, I. Caceres, and M. Gómez-Gesteira. Hybridisation of the wave propagation model SWASH and the meshfree particle method SPH for real coastal applications. *Coastal Engineering Journal*, 57(4):1–34, 2016. ISSN 05785634. doi: 10.1142/S0578563415500242.

C. Altomare, J. Domínguez, A. Crespo, J. González-Cao, T. Suzuki, M. Gómez-Gesteira, and P. Troch. Long-crested wave generation and absorption for sph-based dualsphysics model. *Coastal Engineering*, 127:37–54, 2017.

C. Altomare, B. Tagliafierro, J. Domínguez, T. Suzuki, and G. Viccione. Improved relaxation zone method in sph-based model for coastal engineering applications. *Applied Ocean Research*, 81:15 – 33, 2018. ISSN 0141-1187. doi: https://doi.org/10.1016/j.apor.2018.09.013. URL `http://www.sciencedirect.com/science/article/pii/S0141118718303705`.

B. Bouscasse, S. Marrone, A. Colagrossi, and A. Di Mascio. Multi-purpose interfaces for coupling SPH with other solvers. In *Proceedings of the 8th International SPHERIC Workshop*, Trondheim, 2013.

J. Chicheportiche, V. Hergault, M. Yates, C. Raoult, A. Leroy, A. Joly, and D. Violeau. Coupling SPH with a potential Eulerian model for wave propagation problems. In *Proceedings of the 11th SPHERIC International Workshop*, number 1, pages 246–252, Munich, 2016.

Dean and Dalrymple. *Wavemaker Theory*, pages 170–186. WORLD SCIENTIFIC, 1991. doi: 10.1142/9789812385512_0006.

E. Didier, D. Neves, P. R. F. Teixeira, M. G. Neves, M. Viegas, and H. Soares. Coupling of FLUINCO mesh-based and SPH mesh-free numerical codes for the modeling of wave overtopping over a porous breakwater. In *International Short Course on Applied Coastal Research*, Lisbon, 2013.

G. Fourtakas, P. K. Stansby, B. D. Rogers, S. J. Lind, S. Yan, Q. W. Ma, et al. On the coupling of incompressible sph with a finite element potential flow solver for nonlinear free surface flows. In *The 27th International Ocean and Polar Engineering Conference*. International Society of Offshore and Polar Engineers, 2017.

G. Fourtakas, P. Stansby, B. Rogers, and S. Lind. An Eulerian-Lagrangian incompressible SPH formulation (ELI-SPH) connected with a sharp interface. *Comput. Methods Appl. Mech. Engrg. Comput. Methods Appl. Mech. Engrg*, 329(329):532–552, 2018. doi: 10.1016/j.cma.2017.09.029.

H. Gotoh and A. Khayyer. On the state-of-the-art of particle methods for coastal and ocean engineering. *Coastal Engineering Journal*, 0(0):1–25, 2018. doi: 10.1080/21664250.2018.1436243.

C. Kassiotis, M. Ferrand, D. Violeau, B. Rogers, P. Stansby, M. Benoit, B. D. Rogers, and P. K. Stansby. Coupling SPH with a 1-D Boussinesq-type wave model. In *6th International SPHERIC Workshop*, pages 241–247, Hamburg, 2011.

P. Kumar, Q. Yang, V. Jones, and L. Mccue-Weil. Coupled SPH-FVM simulation within the OpenFOAM framework. *Procedia IUTAM*, 18:76–84, 2015. doi: 10.1016/j.piutam.2015.11.008.

S. Marrone, A. Di Mascio, and D. Le Touzé. Coupling of smoothed particle hydrodynamics with finite volume method for free-surface flows. *Journal of Computational Physics*, 310:161–180, 2016.

E. Napoli, M. De Marchis, C. Gianguzzi, B. Milici, and A. Monteleone. A coupled finite volume–smoothed particle hydrodynamics method for incompressible flows. *Computer Methods in Applied Mechanics and Engineering*, 310:674–693, 2016.

M. Narayanaswamy, A. J. C. Crespo, M. Gómez-Gesteira, and R. A. Dalrymple. Sphysics-funwave hybrid model for coastal wave propagation. *Journal of Hydraulic Research*, 48(S1):85–93, 2010.

B. Ren, M. He, P. Dong, and H. Wen. Nonlinear simulations of wave - induced motions of a freely floating body using WCSPH method. *Applied Ocean Research*, 50:1–12, 2015. doi: 10.1016/j.apor.2014.12.003.

A. Tafuni, J. Domínguez, R. Vacondio, I. Sahin, and A. Crespo. Open boundary conditions for large-scale sph simulations. In *Proceedings of the 11th SPHERIC International Workshop*, 2016.

A. Tafuni, J. M. Domínguez, R. Vacondio, and A. Crespo. Accurate and efficient SPH open boundary conditions for real 3-D engineering problems. In *12th International SPHERIC Workshop*, pages 1–12, Ourense, 2017.

A. Tafuni, J. Domínguez, R. Vacondio, and A. Crespo. A versatile algorithm for the treatment of open boundary conditions in smoothed particle hydrodynamics gpu models. *Computer Methods in Applied Mechanics and Engineering*, 342(1):604–624, 2018. ISSN 0045-7825. doi: https://doi.org/10.1016/j.cma.2018.08.004. URL `http://www.sciencedirect.com/science/article/pii/S0045782518303906`.